# Target-Cell Contact Activates a Highly Selective Capacitative Calcium Entry Pathway in Cytotoxic T Lymphocytes

**Adam Zweifach**

Department of Physiology and Biophysics and Department of Immunology, University of Colorado Health Sciences Center, Denver, Colorado 80262

*Abstract.* Calcium influx is critical for T cell activation. Evidence has been presented that T cell receptor–stimulated calcium influx in helper T lymphocytes occurs via channels activated as a consequence of depletion of intracellular calcium stores, a mechanism known as capacitative $Ca^{2+}$ entry (CCE). However, two key questions have not been addressed. First, the mechanism of calcium influx in cytotoxic T cells has not been examined. While the T cell receptor–mediated early signals in helper and cytotoxic T cells are similar, the physiology of the cells is strikingly different, raising the possibility that the mechanism of calcium influx is also different. Second, contact of T cells with antigen-presenting cells or targets involves a host of intercellular interactions in addition to those between antigen–MHC and the T cell receptor. The possibility that calcium influx pathways in addition to those activated via the T cell receptor may be activated by contact with relevant cells has not been addressed. We have used imaging techniques to show that target-cell–stimulated calcium influx in CTLs occurs primarily through CCE. We investigated the permeability of the CTL influx pathway for divalent cations, and compared it to the permeability of CCE in Jurkat human leukemic T cells. CCE in CTLs shows a similar ability to discriminate between calcium, barium, and strontium as CCE in Jurkat human leukemic T lymphocytes, where CCE is likely to mediated by $Ca^{2+}$ release–activated $Ca^{2+}$ current (CRAC) channels, suggesting that CRAC channels also underlie CCE in CTLs. These results are the first determination of the mechanism of calcium influx in cytotoxic T cells and the first demonstration that cell contact–mediated calcium signals in T cells occur via depletion-activated channels.

Key words: CTL • $Ca^{2+}$ release–activated $Ca^{2+}$ current • Fura-2 • granule exocytosis • perforin

## *Introduction*

$Ca^{2+}$ influx is critical for T cell activation (Berke, 1994; Weiss and Littman, 1994). In helper ($CD4^+$) T cells, $Ca^{2+}$ influx leads to the activation of cytokine genes (Weiss and Littman, 1994), and different patterns of calcium signals can regulate which cytokines are produced (Dolmetsch et al., 1998). In cytotoxic T cells (CTLs),[1] $Ca^{2+}$ influx participates in the exocytosis of lytic granules that contain perforin and granzymes (Berke, 1994). In both T cell types, interaction of antigen–MHC with the T cell receptor (TCR) leads to production of inositol 1,4,5 trisphosphate ($IP_3$) and diacylglycerol (Berke, 1994; Weiss and Littman, 1994). $IP_3$ opens $IP_3$ receptor channels in the ER, causing release of sequestered $Ca^{2+}$, and diacylglycerol activates protein kinase C (PKC). The combination of $Ca^{2+}$ ionophores such as ionomycin or A23187 and PKC activators like phorbol myristate acetate (PMA) can substitute for antigen–MHC in promoting proliferation and cytokine production in $CD4^+$ T cells and proliferation and lytic granule exocytosis in $CD8^+$ cells (Berke, 1994; Weiss and Littman, 1994).

Recent work has provided support for the idea that TCR-dependent $Ca^{2+}$ influx in helper T cells (or lines with helper phenotype) occurs through a class of channels that are activated as a consequence of depletion of the cell's intracellular $Ca^{2+}$ stores (Zweifach and Lewis, 1993; Partiseti et al., 1994; Premack et al., 1994; Fanger et al., 1995), a mechanism known as capacitative $Ca^{2+}$ entry (CCE)

Address correspondence to Dr. Adam Zweifach, Department of Physiology and Biophysics, University of Colorado Health Sciences Center, 4200 East 9th Avenue, Denver, CO 80262. Tel.: (303) 315-5007. Fax: (303) 315-8110. E-mail: adam.zweifach@uchsc.edu

[1]*Abbreviations used in this paper:* APC, antigen-presenting cell; BLT, *N*-(-benzyloxycarbonyl-L-lysine thiobenzyl ester); $[Ca^{2+}]_i$, intracellular calcium; $Ca^{2+}{}_0$, extracellular $Ca^{2+}$; CCE, capacitative $Ca^{2+}$ entry; CRAC, $Ca^{2+}$ release–activated $Ca^{2+}$ current; CTLs, cytotoxic T cells; DTNB, 5,5′-dithio-bis-(2-nitrobenzioic acid); $IP_3$, inositol 1,4,5 trisphosphate; PKC, protein kinase C; PMA, phorbol myristate acetate; SOC, store-operated $Ca^{2+}$ channel; TCR, T cell receptor; TG, thapsigargin.

(Putney, 1990). While other mechanisms have been proposed to participate in $Ca^{2+}$ influx, including $IP_3$-gated channels (Kuno et al., 1986), voltage-gated $Ca^{2+}$ channels (Densmore et al., 1996), and reverse $Na^+$-$Ca^{2+}$ exchange (Wacholtz et al., 1992), evidence has been presented that argues against the involvement of these pathways (for review see Lewis and Cahalan, 1995).

In T cells, store depletion is believed to activate influx via a functionally defined subtype of store-operated channels (SOCs) called $Ca^{2+}$ release-activated $Ca^{2+}$ (CRAC) channels (Zweifach and Lewis, 1993; Partiseti et al., 1994; Premack et al., 1994; Fanger et al., 1995), first identified in Jurkats (Lewis and Cahalan, 1989) and mast cells (Hoth and Penner, 1992). Among the properties of CRAC channels are the following: an inwardly rectifying current-voltage relationship, fast inactivation during hyperpolarizing voltage pulses, a lack of current noise when external divalent cations are present, and a high selectivity for $Ca^{2+}$ over other divalent cations and $Na^+$ (Parekh and Penner, 1997). Selectivity for $Ca^{2+}$ is a key property that distinguishes CRAC channels from other SOCs, as CRAC channels are the only SOCs known that exhibit $Ca^{2+}$ selectivity (Parekh and Penner, 1997). For example, in *Xenopus* oocytes, store depletion activates an inwardly rectifying current that exhibits fast inactivation, but is permeable to $Ca^{2+}$, $Ba^{2+}$, and $Sr^{2+}$ (Yao and Tsien, 1997). A CCE pathway in A431 cells was found to be more permeable to $Ba^{2+}$ than $Ca^{2+}$ (Luckhoff and Clapham, 1994). In vascular endothelial cells, a depletion-activated current was described that was essentially equally permeable to $Ca^{2+}$ and $Ba^{2+}$ (Vaca and Kunze, 1993). In pancreatic acinar cells, a depletion-activated nonselective influx pathway has been described previously (Krause et al., 1996).

The selectivity of CRAC channels for $Ca^{2+}$ over other ions reflects a blocking effect of internal ions (primarily $Mg^{2+}$) that must be knocked out of the pore to allow current flow (Hoth, 1995; Kerschbaum and Cahalan, 1998). $Ca^{2+}$, but not $Ba^{2+}$, can serve this function, and, thus, $Ca^{2+}$ carries sustained currents through CRAC channels whereas $Ba^{2+}$ does not. The most complete analysis of CRAC channel divalent permeation to date was performed by Hoth (1995). He found that switching from $Ca^{2+}$ to $Ba^{2+}$ solutions gave rise to kinetically complex currents and, further, that CRAC channels in Jurkats behaved differently than CRAC channels in mast and rat basophilic leukemia cells. In rat basophilic leukemia cells, $Ba^{2+}$ can actually pass through the pore better than $Ca^{2+}$ because $Ba^{2+}$ currents at some potentials are transiently larger than $Ca^{2+}$ currents. These results suggest that there may be different subtypes of CRAC channels expressed in different cell types. Full understanding of the distinctions between different CCE pathways will require an analysis of the molecular identity of the protein(s) forming the influx pathway. Although there is evidence that homologues of the *Drosophila* trp gene product may form SOCs (see for example Warnat et al., 1999), the molecular basis of CCE in mammalian cells remains unknown.

Despite the progress in understanding the mechanism of TCR-stimulated $Ca^{2+}$ influx, two key issues regarding $Ca^{2+}$ influx in T cells have not been addressed. First, it has not been determined whether CCE is responsible for the $Ca^{2+}$ influx that accompanies granule exocytosis in CTLs. The similarity of upstream signaling events in helper T cells and CTLs might suggest that the $Ca^{2+}$ influx pathway is similar. However, the physiology of the two cell types is sufficiently different that different $Ca^{2+}$ influx pathways might be required. Intracellular $Ca^{2+}$ ($[Ca^{2+}]_i$) levels must be elevated for hours to activate cytokine genes in $CD4^+$ cells (Crabtree, 1989). By contrast, granule-dependent killing by CTLs is an extremely rapid process, occurring in minutes (Poenie et al., 1987; this report), that does not require new gene expression. While several studies have demonstrated that contact of CTLs with appropriate targets leads to an increase in $[Ca^{2+}]_i$, and the contribution of influx to the response has been demonstrated (Gray et al., 1987, 1988; Poenie et al., 1987; Haverstick et al., 1991; Hess et al., 1993), the mechanism of $Ca^{2+}$ influx in CTLs has not been determined.

The second issue that has not been addressed is whether influx pathways in addition to CCE contribute significantly to influx stimulated by contact of a T cell with an antigen-presenting cell (APC) or target. Interactions of T cells with APCs or targets involves a host of intercellular interactions in addition to the binding of antigen–MHC to the TCR. Accessory molecules such as CD3, CD4, and CD8 also interact with antigen–MHC, and adhesion molecules such as LFA-1 and CD2/LFA-2 are known to be critical for APC or target cell binding (Berke, 1994). The involvement of adhesion molecules in T cell interactions with APCs and targets is particularly intriguing, as it has been demonstrated that integrin binding to RGD-containing peptides can trigger a non-CCE pathway in MDCK cells (Sjaastad et al., 1996), and integrin binding has been shown to stimulate $[Ca^{2+}]_i$ increases in Jurkats (Weismann et al., 1997). The adhesion molecule LFA-1 has been shown to activate signaling pathways in CTLs distinct from those activated by the TCR (Ni et al., 1999). Findings such as these raise the possibility that a non-CCE $Ca^{2+}$ influx pathway might be activated in parallel to CCE in T cells stimulated by contact with an APC or target. All studies to date in which the mechanism of calcium influx in T cells has been addressed have relied on mAbs, mitogenic lectins, or store-depleting drugs (Lewis and Cahalan, 1989; Hess et al., 1993; Zweifach and Lewis, 1993; Partiseti et al., 1994; Premack et al., 1994; Fanger et al., 1995). Studies that have demonstrated cell contact–stimulated $[Ca^{2+}]_i$ signals in T cells have not addressed the mechanism(s) of influx (Poenie et al., 1987; Gray et al., 1987, 1988; Donnadieu et al., 1992; Agrawal and Linderman, 1995; Negulescu et al., 1996; Delon et al., 1998).

In the present study we have used imaging techniques to provide evidence that target-cell–stimulated $Ca^{2+}$ influx accompanying CTL lytic granule exocytosis occurs primarily via CCE. Imaging techniques offer advantages over patch clamp techniques for such an investigation, as the conditions required to record CCE, which include high levels of intracellular $Ca^{2+}$ buffers, pipette solutions designed to block contaminating currents and voltage protocols designed to maximize CCE, might obscure the presence of other $Ca^{2+}$ entry pathways. Our results are the first demonstration that CCE can account for $[Ca^{2+}]_i$ signals stimulated by contact of a T cell with a relevant cellular partner. We show that CCE in CTLs displays a similar ability to discriminate between $Ca^{2+}$, $Ba^{2+}$, and $Sr^{2+}$ as

CCE in Jurkat cells, suggesting that CRAC channels may also underlie CCE in CTLs. Significantly, the fact that CCE is responsible for target cell–stimulated $Ca^{2+}$ influx in CTLs indicates that CCE can serve $Ca^{2+}$-dependent T cell functions as diverse as gene expression and lytic granule exocytosis.

## Materials and Methods

### Chemicals and Reagents

Salts for physiological solutions, N-(-benzyloxycarbonyl-L-lysine thiobenzyl ester [BLT]), 5,5′-dithio-bis-(2-nitrobenzioic acid) (DTNB), and poly-L-lysine were purchased from Sigma-Aldrich. Fura-2 AM and calcein AM were from Molecular Probes. Thapsigargin was purchased from Alexis Biochemicals. Anti-CD3 beads (M-450 Pan T) were purchased from Dynal A.S. RPMI 1640 and tissue culture plastic was obtained from Fisher Scientific. FCS, glutamine, and antibiotics were purchased from Gemini Bioproducts. T-stim IL-2 containing conditioned medium was purchased from Becton Dickinson.

### Cells

JY (HLA-A2, -B7, and -Dr4,6). and Jurkat E6-1 cells were maintained in RPMI supplemented with 2 mM glutamine, 10% heat-inactivated FCS, and antibiotics (complete cell culture medium). The AJY CTL line (HLA-A3, B7) was maintained in complete medium supplemented with 15% T-stim. AJYs were given irradiated JYs (10,000 R) once a week (ratio of AJYs to JYs ~10–20:1), and used for experiments 4–6 d after stimulation. JYs and AJYs were the gift of Dr. Carol Claybergher (Stanford University, Stanford, CA); Jurkat E6-1s were provided by Dr. Michael Cahalan (University of California, Irvine, Irvine, CA).

### Solutions

Ringer's solution contained the following (in mM): 145 NaCl, 4.5 KCl, 1 $MgCl_2$, 2 $CaCl_2$, 5 Hepes, and 10 glucose (pH 7.4 with NaOH). Zero $Ca^{2+}$ Ringer's was identical, except $CaCl_2$ was replaced with $MgCl_2$. Zero $Ca^{2+}$ Ringer's plus EGTA was identical to zero $Ca^{2+}$ Ringer's, but was supplemented with 1 mM EGTA. $K^+$-Ringer's contained (in mM): 160 KCl, 1 $MgCl_2$, 2 $CaCl_2$, 5 Hepes, and 10 glucose, pH 7.4 with KOH. $Ca^{2+}$-free $K^+$-Ringer's contained (in mM): 160 KCl, 1 $MgCl_2$, 5 Hepes, and 10 glucose, pH 7.4 with KOH. In experiments with different cations ($Ba^{2+}$, $Sr^{2+}$, and $Mn^{2+}$), a 0.1-M or 1-M stock solution of the chloride salt was prepared in distilled water. For $Mn^{2+}$ quench experiments, $Mn^{2+}$ was added to normal Ringer's. To investigate the permeability of $Ca^{2+}$ entry pathways, $Ba^{2+}$ or $Sr^{2+}$ was added to $Ca^{2+}$-free $K^+$-Ringer's.

### Loading of Cells with Dyes

JYs were loaded with calcein by incubating them with 2.5 μM calcein-AM in cell culture medium for 30 min at room temperature. AJYs were loaded with Fura-2 by incubating them with 1 μM Fura-2 AM in cell culture medium for 30 min at room temperature. Cells were washed twice with fresh medium before use.

### Imaging

Experiments were performed with an imaging system built around a Nikon Diaphot 300 inverted microscope (Nikon Inc.) equipped for epifluorescence. A Nikon PlanFluor 40× oil objective (NA 1.4) was used for all experiments. Excitation light was provided by a 150-W Xenon arc lamp (Optiquip), and was attenuated to 12% for Fura-2 experiments or 1% for calcein experiments using neutral density filters. Excitation wavelength was selected using appropriate excitation filters in a Sutter Lambda-10 filter wheel (Sutter Instruments). A Fura-BCECF dichroic mirror was used in the filter cube, and emission light was filtered with a second Sutter filter wheel. Filters and the dichroic mirror were obtained from Chroma. Images were acquired with a Cooke Sensicam peltier-cooled interline CCD camera (PCO). For Fura-2 experiments, ratios were collected every 6 or 8 s. Exposure times were 150 or 200 ms for F340 and F360, and 75 or 100 ms for F380. Typically, the CCD array was binned 8 × 8 to increase sensitivity and decrease data density. Hardware was controlled and images were acquired and analyzed with SlideBook software from Intelligent Imaging Innovations, Inc., running on a Dell Dimensions Pentium II computer with 500 MB of RAM.

Imaging experiments were conducted at room temperature. The experimental chambers consisted of lids of 35-mm petri dishes in which a 5-mm diam hole was milled and a coverslip was attached to the bottom with Sylgard. The volume of chambers was ~30 μl. This small volume was kept from evaporating by covering the chamber with a lid to which a sponge, wetted with Ringer's, was attached. Solutions were changed using a hand held suction line and a 1-ml pipetter in experiments in which targets were applied, or using fixed-position syringe-driven perfusion inlet and vacuum-driven outlet lines. In either case, because of the extremely small volume of the chamber, solution exchange was complete within 2 s. Coverslips were coated with poly-L-lysine to promote cell adherence.

For analysis of Fura-2 ratio data, background-subtracted images were thresholded on F340, and the ratios were computed pixel-by-pixel for all pixels above threshold. Ratios were converted to estimates of $[Ca^{2+}]_i$ using the method of Grynkiewicz et al. (1985). Calibration values were measured in vitro, assuming a dissociation constant of 300 nM for the binding of $Ca^{2+}$ to Fura-2 (Negulescu et al., 1996). For $Mn^{2+}$ quench experiments, $[Ca^{2+}]_i$ was determined as above, whereas F360 was measured with no thresholding. After initial processing, all fluorescence data were exported to Igor Pro for subsequent analysis.

To align $[Ca^{2+}]_i$ responses (see Fig. 4), an automatic routine was written in Igor Pro. For each cell, resting $[Ca^{2+}]_i$ was computed for the 72-s before addition of JYs. A threshold was set at 50 nM above this value, and the routine automatically detected the first threshold crossing. All points >80 s before the threshold crossing were deleted from the trace, resulting in temporally aligned traces. Another routine written in Igor Pro was used to inspect traces and add them to a running average. After the average was calculated, standard deviations for the data set were computed. Statistical significance of the data in Fig. 5 was computed using an unpaired *t* test.

### BLT-esterase Assays

BLT-esterase activity released from AJYs (Takayama et al., 1987) was measured by resuspending AJYs at a density of $1.6 \times 10^8$ cells/ml of cell culture medium. The cell suspension was pipetted into wells of a v-bottom 96-well microtiter plate (5 μl/ well), and 100 μl of appropriate experimental solution was added to each well (see above for composition). The cells were incubated for 2 h at 37°C in 5% $CO_2$. After the incubation period, the cells were resuspended by careful pipetting, and centrifuged at 200 *g* for 0.5 min. 50 μl of supernatant was transferred to another 96-well plate for analysis of BLT-esterase activity. 75 μl of BLT solution (0.2 mM BLT and 0.22 mM DTNB) in PBS, pH 7.2, was added to the supernatant of each condition. The 96-well plate was covered with parafilm and incubated in the dark at room temperature for 40 min. BLT activity was determined from absorbance measurements made on a Dynatech Minireader II, read at 410 nm after subtraction of an appropriate blank.

The percentage of BLT-esterase release in each experimental condition was calculated as follows:

$$\text{Release (\%)} = \frac{E - S}{T - S} \times 100,$$

where E is the BLT-esterase activity in the supernatant of experimental wells, S is BLT-esterase activity in the supernatant of a well containing normal Ringer's with no stimuli, and T is the total amount of BLT activity determined by adding 0.1% Triton X-100 to cells in normal Ringer's. All determinations were made in triplicate.

## Results and Discussion

### AJYs Kill JYs Using Granule Exocytosis

This study was designed to investigate the mechanism of target-cell–stimulated $Ca^{2+}$ influx accompanying lytic granule exocytosis by CTLs. We chose AJY CTLs, a long-term human HLA-A2 allospecific CTL line, for these studies. Previous work has shown that these cells are $CD8^+$, and that mAbs against CD8, LFA-1, LFA-2, and LFA-3 inhibit lysis of JYs (Koller et al., 1987). We developed a novel imaging technique derived from the calcein-

release assay (CARE-LASS) (Lichtenfels et al., 1994) to confirm that AJYs use granule exocytosis rather than the FAS pathway (Berke, 1994) to kill JYs, and to explore the kinetics of granule exocytosis, as the relevant $[Ca^{2+}]_i$ rise must occur before hitting. Calcein is a membrane-impermeant dye that is well-retained in cells with intact plasma membranes. CARE-LASS measures the amount of calcein released into the extracellular solution from loaded targets to monitor hitting. We reasoned that, as perforin pore formation following granule exocytosis is accompanied by an increased membrane permeability to calcein, we should be able to monitor hitting as a decrease in target cell calcein fluorescence in imaging experiments. JY targets were loaded with calcein-AM, and allowed to adhere to coverslips coated with poly-L-lysine. An excess of AJYs was added to the chamber, and allowed to settle into contact with the JYs. Addition of AJYs in this manner established contact with JYs in ~30–60 s. Fig. 1 shows results from a typical experiment. After a delay, target cells exhibited sudden decreases in calcein fluorescence, consistent with perforin-induced increases in membrane permeability to calcein. The shortest latency observed was ~400 s and the mean latency was 1,031 s. By 2,000 s, ~65% of JYs had lost their fluorescence. Jurkats, which are not targets for JYs, did not demonstrate similar fluorescence decreases when exposed to AJYs (data not shown).

To confirm that the decreases in fluorescence we observed correspond to perforin-induced membrane damage, we repeated the experiment in $Ca^{2+}$-free external solution (Fig. 1 C) as cell killing because of granule exocytosis but not FAS has been shown to depend absolutely on the presence of external $Ca^{2+}$ (Berke, 1994; Griffiths, 1995). In the absence of external $Ca^{2+}$ ($Ca^{2+}{}_0$), sudden decreases in calcein fluorescence were not observed over a period of ~2,000 s. When the external solution was replaced with $Ca^{2+}$-containing Ringer's, decreases in calcein fluorescence occurred within 60 s. We conclude based on the kinetics and $Ca^{2+}{}_0$ dependence of CTL-induced calcein fluorescence changes that AJYs use granule exocytosis to kill JYs.

An alternative imaging technique for monitoring target cell killing based on Fura-2 fluorescence has been reported (Poenie et al., 1987). In preliminary experiments, we used Fura-2 to measure target cell killing, and found that AJYs were capable of causing robust $[Ca^{2+}]_i$ increases in JYs. However, there are three problems associated with the use of Fura-2 to measure target cell killing. First, the earliest signal is an increase in $[Ca^{2+}]_i$ because of $Ca^{2+}$ in-

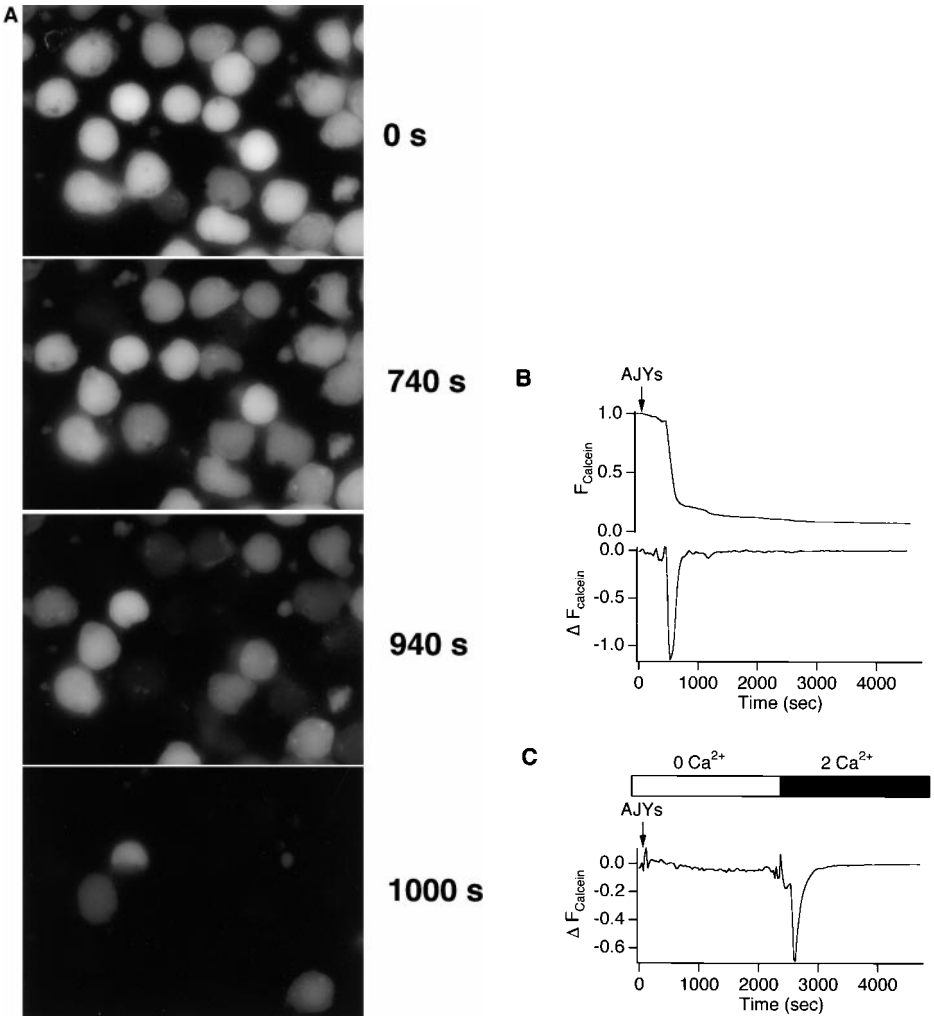


*Figure 1.* AJYs kill JYs rapidly via granule exocytosis. (A) Fluorescence images of calcein-loaded JYs before, 740, 940, and 1,000 s after AJY addition. (B) Representative trace of single-cell calcein fluorescence (top) and differentiated calcein fluorescence (x10, bottom) for one of the cells shown in A. Arrows indicate the addition of JYs. Note the sudden decrease in calcein fluorescence, reflected as a spike in the differentiated traces. (C) Representative differentiated calcein fluorescence from a single cell exposed to AJYs in the absence of $Ca^{2+}{}_0$, followed by perfusion of the chamber with $Ca^{2+}{}_0$. No hitting occurs during the ~2,000 s during which the cell was in $Ca^{2+}$-free solution, but occurs rapidly after addition of $Ca^{2+}{}_0$.

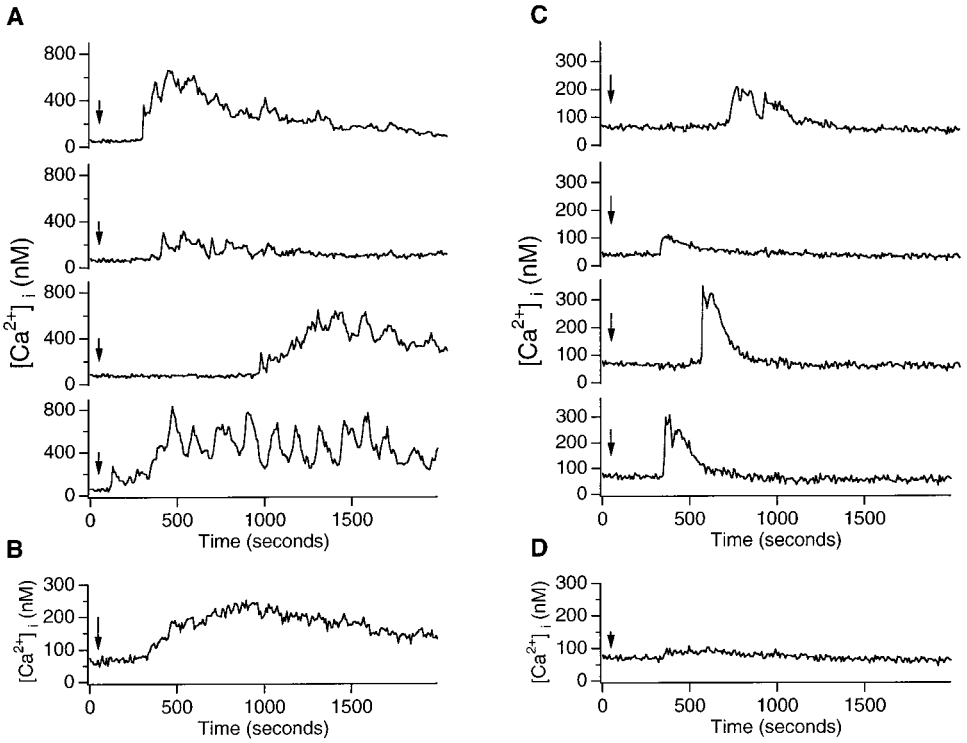


*Figure 2.* $Ca^{2+}$ influx is essential for prolonged $[Ca^{2+}]_i$ signals in CTLs. (A) Four representative traces of single-cell $[Ca^{2+}]_i$ when Fura-2 loaded AJYs were exposed to JYs in the presence of $Ca^{2+}{}_0$. Arrows indicate addition of JYs. $[Ca^{2+}]_i$ responses were extremely variable. (B) Average of all cells in the experiment is shown in A. The average is a poor representation of the single-cell responses. (C) Four representative $[Ca^{2+}]_i$ traces when Fura-2–loaded AJYs were exposed to JYs in the absence of $Ca^{2+}{}_0$. Arrows indicate addition of JYs. (D) Average of all the cells in the experiment shown in C. At the population level, the $[Ca^{2+}]_i$ rise is almost undetectable.

flux through perforin pores; this signal cannot be detected in the absence of $Ca^{2+}{}_0$. Using calcein imaging, we were able to monitor membrane permeability in the presence and absence of $Ca^{2+}{}_0$. Second, because the intensity of Fura-2 fluorescence at both 340 and 380 nm excitation is $Ca^{2+}$-dependent, changes in intensity at these wavelengths cannot unambiguously be attributed to a leak of Fura-2 through perforin channels. Finally, expensive UV-transmitting optics must be used for Fura-2 measurements, and a filter-wheel is required to select excitation wavelengths. As calcein is excited with visible light, standard FITC optics can be used and no filter-wheel is required. We suggest that imaging calcein-loaded targets may be a powerful tool to study the kinetics of hitting at the single-cell level. A further advantage is that comparable population measurements can be conducted in parallel using CARE-LASS.

### *Influx Contributes to $[Ca^{2+}]_i$ Signals in AJYs*

To examine the $[Ca^{2+}]_i$ signals elicited in CTLs by target-cell contact, we loaded AJYs with Fura-2, let them adhere to coverslips coated with poly-L-lysine, and then allowed an excess of JY targets to settle onto them (Fig. 2). Experiments of this sort, originally performed by Poenie et al. (1987), are essentially the converse of the calcein experiments shown in Fig. 1. In these experiments, $[Ca^{2+}]_i$ responses were observed in 62% of cells (172 out of 280 cells from 7 experiments). AJYs exposed to Jurkats in the identical fashion did not exhibit $[Ca^{2+}]_i$ increases (data not shown).

The most striking feature of the $[Ca^{2+}]_i$ responses we observed was their heterogeneity (Fig. 2 A). Both the latency until the onset of a $[Ca^{2+}]_i$ rise and the magnitude and shape of the $[Ca^{2+}]_i$ response were extremely variable (Fig. 2 A). In most cases, the earliest $[Ca^{2+}]_i$ signal consisted of a rapid rise from baseline to ~200–400 nM. The mean latency to the onset of $[Ca^{2+}]_i$ signals was 674 ± 472 s (mean ± SD, $n$ = 172). After this initial response, individual cells displayed very variable responses ranging from a series of small transients to large, sustained oscillations. The mean peak $[Ca^{2+}]_i$ increase was 319 ± 282 nM (mean ± SD, $n$ = 172). Comparison of the mean latency to the initiation of the $[Ca^{2+}]_i$ signal to the mean latency of killing suggests that JY-induced $[Ca^{2+}]_i$ signals precede perforin-induced target cell membrane permeability changes by 300–400 s on average. When tested, ~1,200 s after the addition of JYs, $[Ca^{2+}]_i$ increases in AJYs were reduced when $Ca^{2+}{}_0$ was removed, when extracellular $Na^+$ was replaced by $K^+$, and by application of 5 mM $NiCl_2$ (data not shown). Reduction of $[Ca^{2+}]_i$ after replacement of $Na^+{}_0$ with $K^+{}_0$ provides evidence that influx is not mediated by $Na^+$-$Ca^{2+}$ exchange operating in the reverse mode, as reverse $Na^+$-$Ca^{2+}$ exchange should be enhanced by $Na^+{}_0$ removal, resulting in a decrease in $[Ca^{2+}]_i$. Furthermore, Donnadieu and Trautmann (1993) have presented evidence that macrophages, but not lymphocytes have active $Na^+$-$Ca^{2+}$ exchange, and in macrophages, $Na^+$-$Ca^{2+}$ exchange only functions in the forward mode.

Averaging the single-cell $[Ca^{2+}]_i$ responses ($n$ = 280 cells) results in a trace that is not a good representation of the single-cell behavior (Fig. 2 B), as has been reported previously for Jurkats (Lewis and Cahalan, 1989). Average $[Ca^{2+}]_i$ rises from a resting level of 66 to 236 nM, a difference of 171 nM. Thus, the average behavior, similar to what would be measured in a population assay, underestimates the magnitude of the peak change in $[Ca^{2+}]_i$ by a factor of approximately two.

We confirmed that influx contributes to the $[Ca^{2+}]_i$ elevation by measuring target-cell–induced $[Ca^{2+}]_i$ responses in $Ca^{2+}$-free external solution (Fig. 2 C). Under these conditions, the only source of $Ca^{2+}$ is intracellular stores; differences between $[Ca^{2+}]_i$ responses measured in the presence and absence of $Ca^{2+}{}_0$ reflect the contribution of influx. As in the experiments performed in the presence of $Ca^{2+}{}_0$, ~65% of cells responded (117 out of 180 cells from 6 experiments). In the absence of $Ca^{2+}{}_0$, $[Ca^{2+}]_i$ responses were of a smaller amplitude and shorter duration than in the presence of $Ca^{2+}{}_0$ (Fig. 2 C), which is consistent with previous reports that $Ca^{2+}$ influx plays a role in CTL $[Ca^{2+}]_i$ signals (Poenie et al., 1987; Gray et al., 1987, 1988; Haverstick et al., 1991; Hess et al., 1993). In fact, the $[Ca^{2+}]_i$ signals measured in the absence of $Ca^{2+}{}_0$ were strikingly similar to the earliest responses observed in the presence of $Ca^{2+}{}_0$. The mean peak $[Ca^{2+}]_i$ increase was 153.8 ± 76 nM (mean ± SD, $n$ = 117), approximately half as large as the rise seen in the presence of $Ca^{2+}{}_0$. The latency until responses were initiated was 741 ± 383 s (mean ± SD, $n$ = 117), similar to the results obtained in the presence of $Ca^{2+}{}_0$. This result indicates that early signaling events proximal to release of $[Ca^{2+}]$ from stores occur at the same rate in the presence and absence of $Ca^{2+}{}_0$. Averaging the single-cell $[Ca^{2+}]_i$ responses (Fig. 2 D) underestimates the single-cell responses much more dramatically than in the presence of $Ca^{2+}{}_0$. The average rises from a resting value of 72 to 92 nM, a change of only 20 nM, whereas the single-cell responses show that $[Ca^{2+}]_i$ can actually be sustained at levels of hundreds of nanomolar above baseline for several hundred seconds. The discrepancy between the single-cell behavior and the population behavior in the absence of $Ca^{2+}{}_0$ highlights the importance of single-cell measurements.

### *Release of $Ca^{2+}$ from Intracellular Stores Precedes Influx*

The heterogeneity of the single-cell $[Ca^{2+}]_i$ responses in the presence of $Ca^{2+}{}_0$ (Fig. 2 A) poses a significant challenge to understanding both the relative contribution of influx and its mechanism. However, as stated above, the initial portion of the $[Ca^{2+}]_i$ rise observed in the presence of $Ca^{2+}{}_0$ is strongly reminiscent of the responses observed in the absence of $Ca^{2+}{}_0$, suggesting that the initial phase of the $[Ca^{2+}]_i$ response in the presence of $Ca^{2+}{}_0$ consists of release from stores. Thus, the responses, despite their variability, might consist of release of $Ca^{2+}$ from intracellular stores followed by influx across the plasma membrane.

We used two independent means to examine the relative timing of store release and influx. First, we reasoned that if we temporally aligned $[Ca^{2+}]_i$ responses, then we could remove the latency to the initiation of the $[Ca^{2+}]_i$ rise as a source of heterogeneity in the response. Comparison of averaged aligned traces obtained in the presence or absence of $Ca^{2+}{}_0$ (Fig. 3 A) revealed that the initial portion of the $[Ca^{2+}]_i$ responses is identical, as suggested by the results presented above. Differences between the two conditions become apparent ~80 s after the initiation of $[Ca^{2+}]_i$ responses. The difference between the aligned response obtained in the absence of $Ca^{2+}{}_0$ and that obtained in its presence reflects the average time course of the portion of the $[Ca^{2+}]_i$ rise due to influx (Fig. 3 B), which reaches a maximum ~230 s after the beginning of the response. These data indicate that $[Ca^{2+}]_i$ responses triggered by target-cell contact consist of release of $Ca^{2+}$ from intracellular stores followed after a delay by influx of $Ca^{2+}$ from the extracellular fluid. We suggest that temporal alignment of single-cell $[Ca^{2+}]_i$ data might be a useful tool to remove heterogeneity from other complex responses.

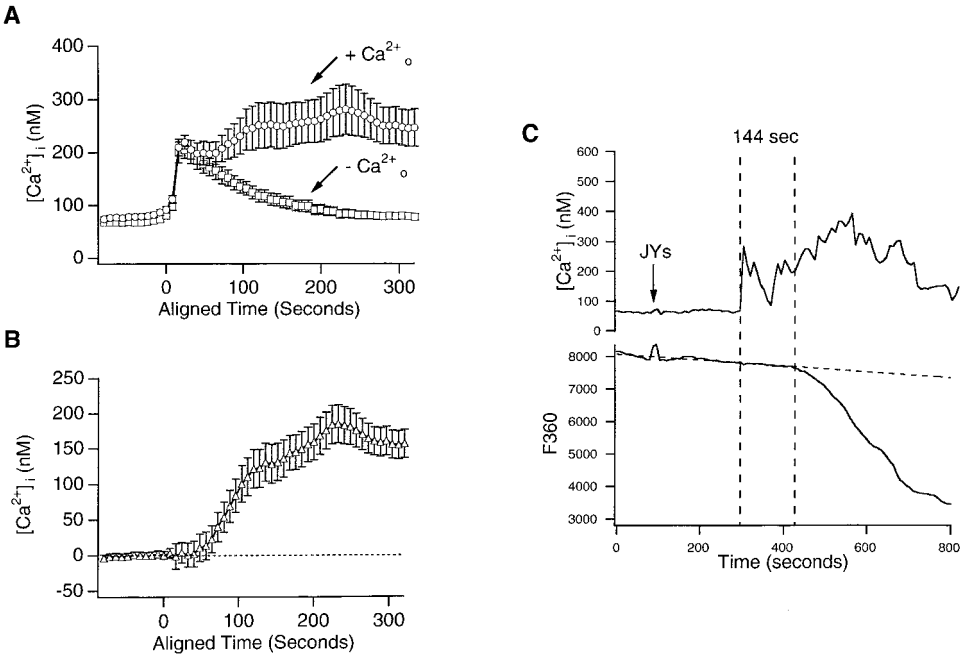


*Figure 3.* Release of $Ca^{2+}$ from intracellular stores precedes influx. (A) Alignment of $[Ca^{2+}]_i$ responses like those shown in Figs. 2 and 3. The earliest portion of the responses are identical. Differences become apparent ~80 s after the initial response. Error bars are 2 SEM, and differences between them thus represent 95% confidence intervals. (B) Computed time course of $Ca^{2+}$ influx obtained by subtracting the aligned 0 $Ca^{2+}$ response from the aligned response in 2 mM $Ca^{2+}$. (C) $Mn^{2+}$ quench allows determination of the relationship between store release and influx in single cells. The top trace is $[Ca^{2+}]_i$ recorded in a single cell after contact with JYs. The bottom trace is F360. 144 s after the initial $[Ca^{2+}]_i$ rise, F360 begins to decrease, demonstrating that influx was activated with a delay in this cell.

The alignment procedure described above allows determination of the average behavior of CTLs. To examine the temporal relationship between release of $Ca^{2+}$ from stores and initiation of influx in single CTLs, we exploited the fact that $Mn^{2+}$ can permeate many $Ca^{2+}$ influx pathways and quench the fluorescence of intracellular Fura-2 (Grynkiewicz et al., 1985; Hallam et al., 1988). In the presence of extracellular $Mn^{2+}$, measuring the fluorescence of Fura-2 at its $Ca^{2+}$-independent isosbestic wavelength (360 nm) in addition to the F340/F380 ratio can, therefore, be used to monitor changes in $[Ca^{2+}]_i$ and influx across the plasma membrane simultaneously (Fig. 3 C).

For these experiments, the extracellular solution was supplemented with 0.5 mM $MnCl_2$, and the fluorescence of Fura-2 excited at 360 nm (F360) was measured in addition to the F340/F380 ratio. Control in vitro experiments demonstrated that F360 changed <10% when $[Ca^{2+}]$ was increased from 0 (10 mM EGTA) to 10 mM. Because AJYs are highly motile cells, it was necessary to conduct these experiments on sparse fields so that the regions of interest used for analysis could entirely contain a given cell at all times. Fig. 3 C shows results of a $Mn^{2+}$ quench experiment. Initially, there was a small slow decline in F360 because of photobleaching. Target cell contact initiated a $[Ca^{2+}]_i$ rise with no significant change in F360. In the cell shown in Fig. 3 C, the rate of decline of F360 increased over its basal level 144 s after the initial increase in $[Ca^{2+}]_i$. These data indicate that the plasma membrane permeability to $Mn^{2+}$ increased detectably at this time, confirming that the release of $Ca^{2+}$ from stores preceded influx. Results compiled from 17 cells indicate that the average delay between release of $Ca^{2+}$ from stores and opening of plasma membrane $Ca^{2+}$ channels was 189 ± 40 s (mean ± SEM). The shortest delay observed was 16 s, whereas the longest was 552 s.

The results of the alignment procedure and of the $Mn^{2+}$ quench experiments both indicate that release of $Ca^{2+}$ from intracellular stores precedes initiation of influx by ~80–200 s. Taken together with the observation that $[Ca^{2+}]_i$ rises precede hitting by 300–400 s, these results suggest that, on average, influx begins ~100–300 s before target-cell hitting. That store release precedes influx is consistent with the idea that target cell-stimulated influx in AJYs occurs via a CCE mechanism.

### *Thapsigargin Stimulates $[Ca^{2+}]_i$ Increases and Granule Exocytosis in CTLs*

We investigated whether AJY CTLs possess CCE by measuring $[Ca^{2+}]_i$ responses to thapsigargin (TG), a drug that activates CCE without generating $IP_3$ in a wide variety of cell types (Fig. 4). Fig. 4 A demonstrates that treatment of cells with 1 μM TG in $Ca^{2+}$-free extracellular solution caused a small transient increase in $[Ca^{2+}]_i$. After the $[Ca^{2+}]_i$ transient has returned to baseline, addition of $Ca^{2+}$ to the external solution results in a large increase in $[Ca^{2+}]_i$. Experiments like the one shown in Fig. 4 A are considered diagnostic of CCE (Putney, 1990), and argue against the participation of a $Ca^{2+}$-activated $Ca^{2+}$ conductance. Maximal $[Ca^{2+}]_i$ was typically higher in cells treated with TG as compared with cells stimulated by contact with targets, likely reflecting the greater degree of store depletion that

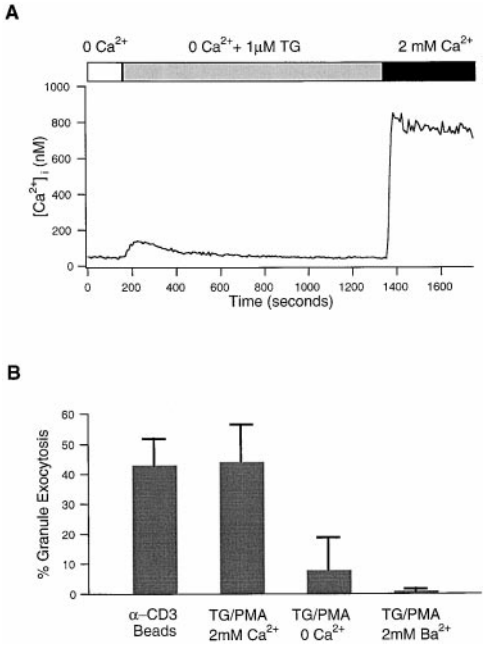


*Figure 4.* Thapsigargin stimulates influx and granule exocytosis. (A) $[Ca^{2+}]_i$ signals in response to application of 1 μM thapsigargin. TG was applied in 0 $Ca^{2+}$ Ringer's, causing a transient increase in $[Ca^{2+}]_i$. When $[Ca^{2+}]_i$ had returned to baseline, perfusion of the chamber with 2 mM $Ca^{2+}{}_0$ caused a large increase in $[Ca^{2+}]_i$ because of the influx. Trace is the average of 40 cells from a single experiment, and is representative of many such experiments. (B) BLT-esterase assays demonstrate that TG + PMA can stimulate granule exocytosis as effectively as anti-CD3–coated beads. TG + PMA stimulated granule exocytosis requires $Ca^{2+}{}_0$. Results are mean + SD from two identical experiments performed in triplicate.

occurs in TG-treated cells. As was the case with target-cell stimulation, and as has been reported for Jurkat human leukemic T cells (Lewis and Cahalan, 1989), TG-stimulated $[Ca^{2+}]_i$ responses were dependent on the presence of $Ca^{2+}{}_0$, inhibited when extracellular $Na^+$ was replaced by $K^+$, and blocked by 5 mM $NiCl_2$ (data not shown). As stated above, reduction of $[Ca^{2+}]_i$ after replacement of $Na^+{}_0$ with $K^+{}_0$ provides evidence that influx is not mediated by $Na^+$-$Ca^{2+}$ exchange operating in the reverse mode.

If target-cell contact stimulates $Ca^{2+}$ influx through CCE, then treatment of cells with TG + PMA should be able to stimulate granule exocytosis. We confirmed that treating AJYs with TG + PMA can stimulate granule exocytosis using BLT-esterase assays (Takayama et al., 1987) (Fig. 4 B). These assays measure the release of granzyme A from CTLs and, thus, allow determination of exocytosis in CTL populations. TG in combination with PMA was as effective as anti-CD3 coated beads at promoting granzyme release. Anti-CD3 beads caused $[Ca^{2+}]_i$ signals that were similar to those caused by target-cell contact (data not shown). We were unable to perform BLT-esterase assays using JYs to stimulate AJYs because JYs have an esterase activity that reacts with the BLT substrate (data not shown). TG/PMA–stimulated granule exocytosis was re-

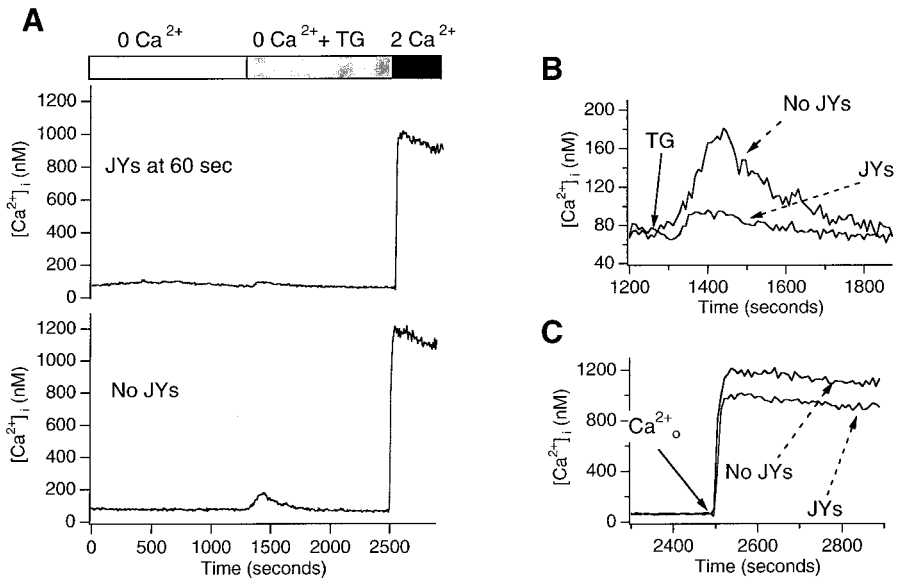


*Figure 5.* Contact with JYs depletes TG-sensitive stores, but does not increase the rate or extent of influx over that observed when AJYs are stimulated with TG alone. (A) Overview of the experiment. Fura-2–loaded AJYs in 0 $Ca^{2+}$ Ringer's were or were not exposed to JYs. At 1,288 s, 1 μM TG was applied in 0 $Ca^{2+}$ Ringer's. Finally, at 2,496 s, normal Ringer's was applied. (B) Expanded view of t = 1,200–1,870 s. Cells that responded to JYs released less $Ca^{2+}$ from TG-sensitive stores than cells that were never exposed to JYs. (C) Expanded view of t = 2,300–2,900 s. When normal Ringer's was applied, the rate of rise of $[Ca^{2+}]_i$ and peak $[Ca^{2+}]_i$ were lower in cells that had responded to JYs. Traces are the average of 72 cells from 3 experiments for JY + TG stimulation, and 83 cells from 3 experiments for TG stimulation.

duced in the absence of extracellular $Ca^{2+}$. $Ba^{2+}$ could not substitute for $Ca^{2+}$ in promoting granule release.

### *CCE Is the Major Influx Pathway Activated by Target-Cell Contact*

The results presented above indicate that CTLs possess a CCE pathway. We would expect target cell contact to activate CCE, as the data presented in Fig. 2 B demonstrate that target cell contact causes release of $Ca^{2+}$ from intracellular stores. We performed two experiments to explore whether target cell contact activates non-CCE pathways as well as CCE. First, we compared the magnitude of $Ca^{2+}$ influx in cells that were stimulated with JYs followed by TG versus cells that were stimulated with TG alone (Fig. 5). We reasoned that, if contact with JYs activates CCE and non-CCE pathways, then there would be more influx in cells stimulated with JYs + TG than cells stimulated with TG alone. Second, we compared the relative abilities of $Ca^{2+}$, $Ba^{2+}$, and $Sr^{2+}$ to cause Fura-2 ratio changes in cells stimulated with TG, JYs, or JYs + TG (Fig. 6). We reasoned that, if contact with JYs activates CCE and non-CCE pathways, there should be a difference in divalent cation permeabilities in cells stimulated with TG as compared with cells stimulated with JYs or JYs + TG.

To assess $Ca^{2+}$ influx after JY + TG stimulation, JY targets were dropped onto Fura-2–loaded CTLs in the absence of $Ca^{2+}_0$ as in Fig. 2 C. After 1,300 s, 1 μM TG was applied. Finally, after 2,496 s the chamber was perfused with 2 mM $Ca^{2+}_0$, and the initial slope of the averaged $[Ca^{2+}]_i$ rise and the peak $[Ca^{2+}]_i$ were used as measures of the amount of influx activated. In these experiments, as in the ones shown in Fig. 2, A and C, ~65% of AJYs exhibited $[Ca^{2+}]_i$ responses to JY targets. Only cells that exhibited JY-stimulated $[Ca^{2+}]_i$ rises were included in the average. The $[Ca^{2+}]_i$ rise that follows JY addition is extremely small as a consequence of averaging (Fig. 2 D.) To assess responses to TG stimulation alone, the identical protocol was used except that AJYs were never exposed to JY targets.

Comparison of the average $[Ca^{2+}]_i$ responses of AJYs that responded to targets with those that were never exposed to targets revealed two key results. First, cells that exhibited $[Ca^{2+}]_i$ responses to JY targets released less $Ca^{2+}$ when subsequently stimulated with TG than cells that were not exposed to targets (Fig. 5 B). The peak $[Ca^{2+}]_i$ increase because of TG-stimulated release in cells that responded to JYs was 20 nM, as compared with 107 nM for cells that were never exposed to JYs ($P < 0.0005$). Cells that responded to JYs also released less $Ca^{2+}$ when treated with TG than cells in the same experiment that did not respond to targets (data not shown). These results con-

*Table I. Relative Permeability of Influx in AJY CTLs and Jurkat Leukemic T Cells*

| Cell type | AJY | AJY | AJY | Jurkat | Jurkat |
|---|---|---|---|---|---|
| Stimulation | Thapsigargin | Target cells | Target cells + thapsigargin | Thapsigargin | Digitonin |
| Divalent: | | | | | |
| $Ca^{2+}$ | 1 | 1 | 1 | 1 | 1 |
| $Sr^{2+}$ | 0.083 | 0.11 | 0.094 | 0.06 | 0.42 |
| | (0.076–0.091) | (0.10–0.12) | (0.06–0.13) | (0.048–0.072) | |
| $Ba^{2+}$ | 0.031 | 0.043 | 0.023 | 0.022 | 0.37 |
| | (0.028–0.032) | (0.037–0.049) | (0.02–0.027) | (0.020–0.023) | |

Values are relative slopes determined from the data of Figs. 6 and 7. Numbers in parentheses below are minimum and maximum relative slopes calculated from the standard deviation of the fitted slopes.

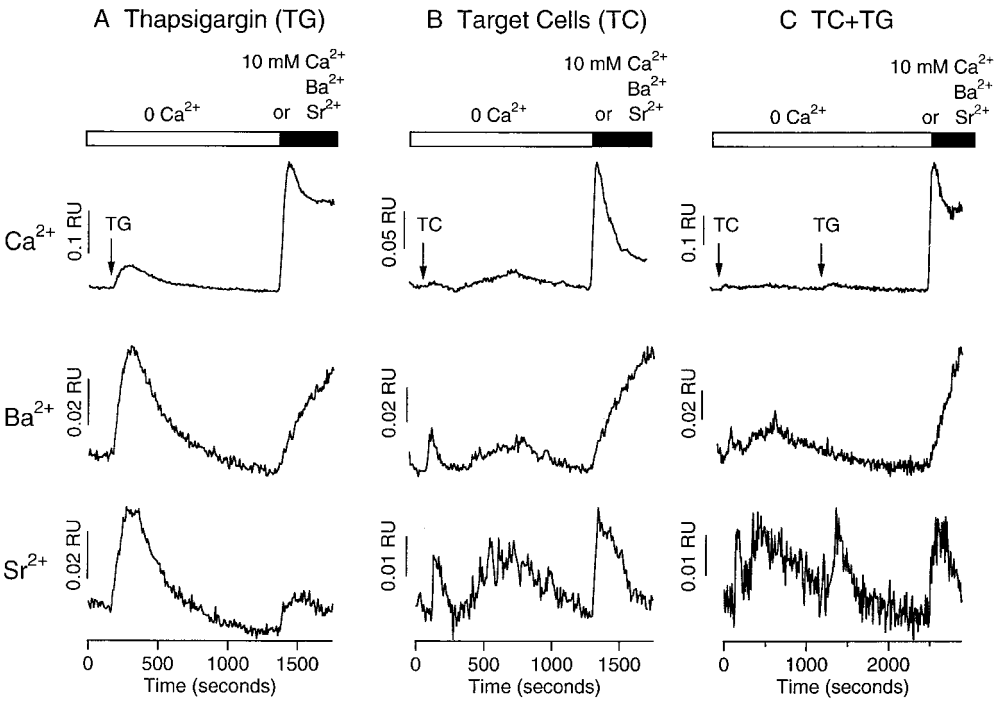


*Figure 6.* AJYs stimulated with TG, JYs, or JYs + TG exhibit identical patterns of divalent cation permeability. (A) Fura-2–loaded AJYs were stimulated with TG in 0 $Ca^{2+}$ $K^+$-Ringer's. Ratio changes in response to application of 10 mM $Ca^{2+}$, $Ba^{2+}$, or $Sr^{2+}$ in $K^+$-Ringer's were measured. Traces are the average of 128 cells from 3 experiments for $Ca^{2+}$, 161 cells from 3 experiments for $Ba^{2+}$, and 132 cells from 3 experiments for $Sr^{2+}$. (B) Fura-loaded AJYs were exposed to JYs in 0 $Ca^{2+}$ $K^+$-Ringer's, followed by addition of $K^+$-Ringer's containing 10 mM $Ca^{2+}$, $Ba^{2+}$, or $Sr^{2+}$. Traces are the average of 127 cells from 7 experiments for $Ca^{2+}$, 110 cells from 9 experiments for $Ba^{2+}$ and 94 cells from 7 experiments for $Sr^{2+}$. (C) Fura-loaded AJYs were exposed to JYs in 0 $Ca^{2+}$ $K^+$-Ringer's, followed by treatment with TG. After 2,496 s, the chamber was perfused with $K^+$-Ringer's containing 10 mM $Ca^{2+}$, $Ba^{2+}$, or $Sr^{2+}$. Traces are the average of 105 cells from 5 experiments for $Ca^{2+}$, 114 cells from 5 experiments for $Ba^{2+}$, and 69 cells from 5 experiments for $Sr^{2+}$. Vertical bars are in ratio units (RU).

firm that contact with JY targets releases $Ca^{2+}$ from the TG-sensitive $Ca^{2+}$ stores that control CCE, which is consistent with the idea that CCE participates in the response to target cells. Critically, the slope of the $[Ca^{2+}]_i$ rise after $Ca^{2+}{}_0$ addition was not higher (in fact, it was slightly lower) in cells that responded to JYs than in cells that were not exposed to JYs, although the difference was not significant. Additionally, peak $[Ca^{2+}]_i$ levels were lower in cells that responded to JYs (967 nM for cells that responded to JYs versus 1,201 nM for cells that were not exposed to JYs, $P < 0.005$; Fig. 5 C). If target-cell contact activated a second influx pathway, we would expect that both the slope of the $[Ca^{2+}]_i$ increase and the peak $[Ca^{2+}]_i$ would be higher in cells that responded to targets as compared with cells that were not exposed to targets. Thus, the data presented in Fig. 5 suggest that target-cell contact does not open any channels other than those activated by store depletion. The lower slope and peak $[Ca^{2+}]_i$ in cells stimulated with JYs + TG may reflect PKC inhibition of the channels (Parekh and Penner, 1995), caused by TCR engagement.

We exploited the fact that the fluorescence of Fura-2 is sensitive to the binding of cations other than $Ca^{2+}$ to compare the permeability properties of the influx pathway(s) stimulated by TG, JYs, or JYs + TG. These methods are expected to activate CCE alone (TG) or CCE and non-CCE pathways (JYs and JYs + TG), as Fig. 5 demonstrates that contact with JYs in $Ca^{2+}$-free external solution depletes the TG-sensitive stores. Activation of a non-CCE pathway should change the relative abilities of $Ca^{2+}$, $Ba^{2+}$, and $Sr^{2+}$ to enter cells, unless the CCE and non-CCE pathways have identical divalent cation permeabilities. We initially tested the ability of a panel of cations to cause ratio changes after TG stimulation. We found that $Ca^{2+}$, $Cd^{2+}$, $Sr^{2+}$, and $Ba^{2+}$ caused ratio increases. However, $Cd^{2+}$ caused ratio increases in unstimulated cells, an effect that may be related to the known toxic effects of $Cd^{2+}$ on lymphocytes (Steffenson et al., 1994). Therefore, we restricted further experiments to $Ca^{2+}$, $Ba^{2+}$, and $Sr^{2+}$.

To determine the divalent cation permeability of CCE in AJYs, cells were treated with 1 μM TG in $Ca^{2+}$-free $K^+$-Ringer's solution to deplete stores maximally and activate influx (Fig. 6 A). After 1,368 s, the chamber was perfused with $K^+$-Ringer's containing 10 mM $Ca^{2+}$, $Ba^{2+}$, or $Sr^{2+}$. $K^+$-Ringer's was used in all divalent cation experiments to clamp the membrane potential, a critical component of the driving force for cation entry, to near 0 mV. We analyzed the initial slope of the averaged ratio increase and found that the sequence of divalent cation–induced ratio changes in AJYs stimulated with TG alone was $Ca^{2+}(1) > Sr^{2+}(0.083) > Ba^{2+}(0.031)$ (Table I). As will be discussed below, these results are consistent with an influx pathway that is highly selective for $Ca^{2+}$.

To assess the divalent cation permeability of target-cell–stimulated influx (Fig. 6 B), JYs were dropped onto Fura-loaded AJYs in $Ca^{2+}$-free $K^+$-Ringer's. After 1,168 s, the chamber was perfused with $K^+$-Ringer's containing 10 mM $Ca^{2+}$, $Ba^{2+}$, or $Sr^{2+}$. Note that, based on the results of Fig. 5 indicating that target–cell contact depletes TG-sensitive stores, we expect target–cell contact to activate CCE in addition to any non-CCE pathways. The initial slope of cation-induced ratio changes followed the sequence $Ca^{2+}(1) > Sr^{2+}(0.11) > Ba^{2+}(0.043)$, similar to the results obtained with TG stimulation. Note that ratio changes

produced by $Ca^{2+}$ addition were smaller and more transient in CTLs stimulated with JYs than cells stimulated with TG (Fig. 6 B), indicating that both the peak and steady-state $[Ca^{2+}]_i$ were lower. This result is consistent with the idea that target-cell contact activates influx via a CCE pathway, as an increase in $[Ca^{2+}]_i$ would be expected to promote store refilling, which has been shown to inactivate CCE in several cell types including lymphocytes (Jacob, 1990; Zweifach and Lewis, 1995). The relatively lower $Ca^{2+}$ slope observed in target-cell–stimulated AJYS might cause a systematic error, leading us to overestimate the relative $Ba^{2+}/Ca^{2+}$ and $Sr^{2+}/Ca^{2+}$ ratios for target-cell stimulation.

We also measured the permeability of influx stimulated by JYs + TG (Fig. 6 C), which like stimulation with JYs, should activate CCE and non-CCE pathways. JYs were dropped onto Fura-loaded AJYs as above. After 1,264 s, the chamber was perfused with $Ca^{2+}$-free $K^+$-Ringer's + 1 μM TG. Finally, after an additional 1,232 s, the chamber was perfused with $K^+$-Ringer's containing 10 mM $Ca^{2+}$, $Ba^{2+}$, or $Sr^{2+}$. The initial slope of cation-induced ratio changes followed the sequence $Ca^{2+}(1) > Sr^{2+}(0.094) > Ba^{2+}(0.028)$, which is similar to the results obtained with targets or TG alone. The similarity of the sequence of divalent cation–induced ratio changes in cells stimulated with TG, JYs, or JYs + TG, taken together with observation that cells stimulated with JYs + TG do not exhibit a higher influx rate than cells stimulated with TG alone, indicates that contact with targets does not activate a significant influx pathway in parallel to CCE.

### *Divalent Cation Permeability of CCE in Jurkats Is Similar to CCE in AJYs*

On the basis of the results presented thus far, we conclude that CCE is the only significant $Ca^{2+}$ influx pathway stimulated by target-cell contact in CTLs. Whereas several different channel types mediating CCE have been reported (Parekh and Penner, 1997), a significant body of evidence suggests that CRAC channels mediate CCE in helper ($CD4^+$) T lymphocytes or lines with helper phenotype such as Jurkat human leukemic T cells (Lewis and Cahalan, 1995). As described in the Introduction, a key property distinguishing CRAC channels from other CCE channels is that they are highly selective for $Ca^{2+}$ over other divalent cations (Clapham, 1995; Parekh and Penner, 1997). CRAC channels are unique in their $Ca^{2+}$ selectivity among all CCE pathways described to date. Therefore, we investigated the pattern of divalent cation permeability in Jurkats (Fig. 7), and compared it to the pattern of divalent cation permeability that we determined for CTLs. We stimulated Jurkats with 1 μM TG in $Ca^{2+}$-free $K^+$-Ringer's. After 1,368 s, we perfused the experimental chamber with $K^+$-Ringer's containing 10 mM $Ca^{2+}$, $Ba^{2+}$, or $Sr^{2+}$ (Fig. 7 A). The ability of the test cations to cause ratio changes was $Ca^{2+}(1) > Sr^{2+}(0.06) > Ba^{2+}(0.023)$, within a factor of two of the results obtained with AJYs.

We confirmed that Fura-2 can detect differences in selectivity of different influx pathways by inducing nonselective influx using the detergent digitonin. We treated Jurkats with 4 μM digitonin in $Ca^{2+}$-free Ringer's solution

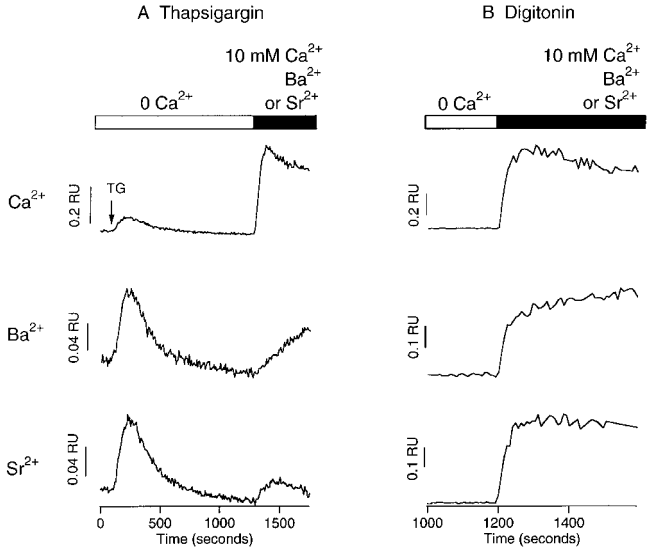


*Figure 7.* The pattern of divalent cation permeability in AJYs is similar to that of $I_{CRAC}$ in Jurkat cells. (A) Fura-2–loaded Jurkats were stimulated with TG in 0 $Ca^{2+}$-$K^+$-Ringer's. Ratio changes in response to application of 10 mM $Ca^{2+}$, $Ba^{2+}$, or $Sr^{2+}$ in $K^+$-Ringer's were measured. Traces are the average of 255 cells from 3 experiments for $Ca^{2+}$, 195 cells from 3 experiments for $Ba^{2+}$, and 222 cells from 3 experiments for $Sr^{2+}$. Ratio changes caused by application of $Ba^{2+}$ and $Sr^{2+}$ were similar to those observed in AJYs. (B) Fura-2–loaded Jurkats were exposed to 4 μM digitonin in $Ca^{2+}$-free Ringer's. After 1,152 s, the chamber was perfused with $Ca^{2+}$-free Ringer's containing 2 mM $Ca^{2+}$, $Ba^{2+}$, or $Sr^{2+}$. Traces are the average of 166 cells from 3 experiments for $Ca^{2+}$, 115 cells from 3 experiments for $Ba^{2+}$, and 140 cells from 3 experiments for $Sr^{2+}$. The pattern of ratio changes is strikingly different than observed after TG stimulation.

(Fig. 7 B). Under these conditions, the membrane is first made permeable to divalent cations before it is made permeable to Fura-2, as determined by simultaneously measuring the F340/F380 ratio and F360 (data not shown). After 1,152 s, we perfused the chamber with $Ca^{2+}$-free Ringer's containing 10 mM $Ca^{2+}$, $Ba^{2+}$, or $Sr^{2+}$. We found that the slope of ratio changes in digitonin-treated Jurkats followed the sequence $Ca^{2+}(1) > Sr^{2+}(0.42) > Ba^{2+}(0.37)$, which is very different than the results with TG. These results confirm that Fura-2 can be used to discriminate selective from nonselective divalent cation influx, and indicate that CCE in CTLs is 7 times as selective for $Ca^{2+}$ over $Sr^{2+}$ and 17 times as selective for $Ca^{2+}$ over $Ba^{2+}$ as digitonin-induced nonselective influx.

Divalent cation–induced fluorescence changes can be affected by a number of factors, including the dissociation constant and maximum ratio of Fura-2, the properties of intracellular buffers, and whether the cation is extruded by plasma membrane ATPases. However, if these factors are similar in AJYs and Jurkats, then the similarity of CCE-stimulated divalent cation–induced fluorescence changes in the two cell types would provide evidence that CCE in the two cells has similar abilities to discriminate between divalent cations. To determine whether divalent cations can induce similar fluorescence changes in AJYs and Jurkats, we induced nonselective influx by treating cells with 4 μM digitonin in the presence of 10 mM $Ca^{2+}$, $Ba^{2+}$, or

$Sr^{2+}$ (data not shown). We measured the F340/F380 ratio, as well as F360 to monitor the progress of permeabilization. Within ~200 s of digitonin treatment, cells began to display ratio increases in the presence of all of the cations. The maximum ratios observed were as follows: $Ca^{2+}(1.0) > Ba^{2+}(0.76) > Sr^{2+}(0.54)$ in Jurkats and $Ca^{2+}(0.77) > Ba^{2+}(0.75) > Sr^{2+}(0.54)$ in AJYs. These results suggest that Fura-2 behaves similarly, but not identically, in the two cell types, as $Ca^{2+}$ gives a smaller maximum ratio in AJYs than in Jurkats. This suggests that our results may underestimate the $Ba^{2+}/Ca^{2+}$ and $Sr^{2+}/Ca^{2+}$ ratios for Jurkats by ~30% compared with AJYs. Correcting for this effect would make the results from Jurkats and AJYS more similar. We conclude that CCE in Jurkats and CTLs is similarly highly selective for $Ca^{2+}$ over $Ba^{2+}$ and $Sr^{2+}$.

### *Significance*

We have demonstrated that target cells activate $Ca^{2+}$ influx in CTLs primarily via CCE. The evidence for these conclusions can be summarized as follows. $[Ca^{2+}]_i$ responses in AJYs consist of both release from intracellular stores and influx, and release of $Ca^{2+}$ from intracellular stores precedes influx, as required if influx occurs through depletion-activated channels. AJY CTLs possess capacitative $Ca^{2+}$ entry as demonstrated by the ability of TG to stimulate robust $[Ca^{2+}]_i$ increases, and contact with target cells depletes the TG-sensitive $Ca^{2+}$ store, as required if target-cell–stimulated $Ca^{2+}$ entry occurs via depletion-activated channels. Two tests for the existence of non-CCE pathways gave negative results. The amount of influx was not higher in cells stimulated with both JYs and TG than in cells stimulated by TG alone, and there was no difference in the divalent cation permeability of influx stimulated by target cells, TG, or the combination of TG and target-cell contact. Note that we cannot entirely rule out minor participation by an additional $Ca^{2+}$ influx pathway.

We have demonstrated that CCE in CTLs has a similar degree of selectivity for $Ca^{2+}$ over $Sr^{2+}$ and $Ba^{2+}$ as CCE in Jurkats, which is believed to occur via CRAC channels (Lewis and Cahalan, 1995). We have as yet been unable to detect the CCE pathway in CTLs in patch clamp experiments, largely because of the presence of a contaminating inwardly rectifying current carried by monovalent cations (Zweifach, A., unpublished observations). Electrophysiological recordings of the CCE current in CTLs would allow determination of such properties as the I-V relationship, amount of current noise, and inactivation properties of the influx pathway, thus providing further points of comparison with $I_{CRAC}$. However, as described in the Introduction, these properties are not unique to CRAC channels, and may, therefore, not be good discriminators between CCE pathways. As $I_{CRAC}$ is the only CCE pathway described to date that is selective for $Ca^{2+}$ over $Ba^{2+}$ and $Sr^{2+}$, our results suggest that CCE in CTLs is mediated by CRAC channels, although it is possible that there are $Ca^{2+}$-selective CCE pathways that are not CRAC that have not yet been discovered.

Our results are significant for three reasons. First, we have shown that target-cell–stimulated $Ca^{2+}$ influx in CTLs occurs primarily via CCE. Previous work has demonstrated $Ca^{2+}$ influx in CTLs in response to target-cell contact, but has not addressed its mechanism. Second, this report is the first time it has been demonstrated that contact of a T cell with a relevant cellular partner activates influx primarily via CCE. Previous studies in which the mechanism of influx in T cells has been addressed used mAbs (Hess et al., 1993; Partiseti et al., 1994; Premack et al., 1994), mitogenic lectins (Lewis and Cahalan, 1989; Zweifach and Lewis, 1993), or pharmacological agents like TG (Zweifach and Lewis, 1993; Premack et al., 1994) to stimulate cells. In studies in which contact-mediated $[Ca^{2+}]_i$ signals have been reported, the mechanism of influx was not determined (Gray et al., 1987, 1988; Poenie et al., 1987; Donnadieu et al., 1992; Agrawal and Linderman, 1995; Negulescu et al., 1996; Delon et al., 1998). Our results rule out the possibility that a significant non-CCE influx pathway is activated by one of the many different cell surface molecules that participate in interactions between T cells and APCs or targets (Berke, 1994; Ni et al., 1999). The third significant finding of this study is that CCE is able to play very diverse roles in T cell physiology. In helper T cells, CRAC channel activity over a period of hours plays a key role in activation of cytokine genes.

Our results demonstrate that CCE, likely also mediated by CRAC channels, can contribute to a very different and much more rapid T cell behavior, i.e., exocytosis of lytic granules. Work on excitable cells has shown that voltage-gated $Ca^{2+}$ channels play roles in processes as diverse as vesicle exocytosis and gene transcription (Ghosh and Greenberg, 1995). The present work demonstrates that CCE plays similarly diverse roles in T cells.

This work would not have been possible without the superb technical assistance of Georjeana A. Burgett. We wish to thank Drs. Carol Clayberger and Shu-Chen Lyu (Stanford University, Stanford, CA) for providing us with AJYs and JYs, and spending an inordinate amount of time helping us learn to culture them. We also thank Drs. Joseph K. Angleson, Dermot F. Cooper, S. Rock Levinson, Diego Restrepo (UCHSC, Denver, CO), Richard S. Lewis (Stanford University, Stanford, CA), and Chris M. Fanger (University of California, Irvine, Irvine, CA), for their helpful comments.

This work was supported by grant AI42964 from the National Institute of Allergy and Immunology.

Submitted: 25 June 1999
Revised: 23 November 1999
Accepted: 21 December 1999

#### *References*

Agrawal, N.G.B., and J.J. Linderman. 1995. Calcium response of helper T lymphocytes to antigen-presenting cells in a single-cell assay. *Biophys. J.* 69: 1178–1190.

Berke, G. 1994. The binding and lysis of target cells by cytotoxic lymphocytes: molecular and cellular aspects. *Annu. Rev. Immunol.* 12:736–753.

Clapham, D. 1995. Calcium signalling. *Cell.* 80:259–268.

Crabtree, G.R. 1989. Contingent genetic regulatory events in T lymphocyte activation. *Science.* 243:355–361.

Delon, J., N. Bercovici, G. Raposo, R. Liblau, and A. Trautmann. 1998. Antigen-dependent and-independent calcium responses triggered in T cells by dendritic cells compared with B cells. *J. Exp. Med.* 188:1473–1484.

Densmore, J., D. Haverstick, G. Szabo, and L. Gray. 1996. A voltage-operable current is involved in $Ca^{2+}$ entry in human lymphocytes whereas ICRAC has no apparent role. *Am. J. Physiol.* 271:C1494–C1503.

Dolmetsch, R.E., K. Xu, and R.S. Lewis. 1998. Calcium oscillations increase the efficiency and specificity of gene expression. *Nature.* 392:933–936.

Donnadieu, E., and A. Trautmann. 1993. Is there a $Na^{+}/Ca^{2+}$ exchanger in macrophages and lymphocytes? *Pflügers Arch.* 424:448–455.

Donnadieu, E., D. Cefai, Y.P. Tan, G. Paresys, G. Bismuth, and A. Trautmann. 1992. Imaging early steps of human T cell activation by antigen-presenting cells. *J. Immunol.* 148:2643–2653.

Fanger, C.M., M. Hoth, G.R. Crabtree, and R.S. Lewis. 1995. Characterization of T cell mutants with defects in capacitative calcium entry: genetic evidence for the physiological roles of CRAC channels. *J. Cell Biol.* 131:655–667.

Ghosh, A., and M.E. Greenberg. 1995. Calcium signaling in neurons: molecular mechanisms and cellular consequences. *Science*. 268:239–247.

Gray, L.S., J.R. Gnarra, and V.H. Engelhard. 1987. Demonstration of a calcium influx in cytolytic T lymphocytes in response to target cell binding. *J. Immunol.* 138:63–69.

Gray, L.S., J.R. Gnarra, J.A. Sullivan, G.L. Mandell, and V.H. Engelhard. 1988. Spatial and temporal characterstics of the increase in intracellular calcium induced in cytotoxic T lymphocytes by cellular antigen. *J. Immunol.* 141: 2424–2430.

Griffiths, G.M. 1995. The cell biology of CTL killing. *Curr. Opin. Immunol.* 7:343–348.

Grynkiewicz, G., M. Poenie, and R.Y. Tsien. 1985. A new generation of $Ca^{2+}$ indicators with greatly improved fluorescence properties. *J. Biol. Chem*. 260: 3440–3450.

Hallam, T.J., R. Jacob, and J.E. Merritt. 1988. Evidence that agonists stimulate bivalent-cation influx into human endothelial cells. *Biochem. J.* 255:179–184.

Haverstick, D.M., V.H. Engelhard, and L.S. Gray. 1991. Three intracellular signals for cytotoxic T lymphocyte-mediated killing: independent roles for protein kinase C, calcium influx, and calcium release from intracellular stores. *J. Immunol.* 146:3306–3313.

Hess, S.D., M. Oortgiesen, and M.D. Cahalan. 1993. Calcium oscillations in human T and natural killer cells depend on membrane potential and calcium influx. *J. Immunol.* 150:2620–2633.

Hoth, M. 1995. Calcium and barium permeation through calcium release-activated calcium (CRAC) channels. *Pflügers Archiv*. 430:315–322.

Hoth, M., and R. Penner. 1992. Depletion of intracellular calcium stores activates a calcium current in mast cells. *Nature*. 355:353–356.

Jacob, R. 1990. Agonist-stimulated divalent cation entry into single cultured human umbilical vein endothelial cells. *J. Physiol.* 421:55–77.

Kerschbaum, H., and M. Cahalan. 1998. Monovalent permeability, rectification, and ionic block of store-operated calcium channels in Jurkat T lymphocytes. *J. Gen. Physiol.* 111:521–537.

Koller, T.D., C. Clayberger, J.L. Maryanski, and A.M. Krensky. 1987. Human allospecific cytolytic T lymphocyte lysis of a murine cell transfected with HLA-A2. *J. Immunol.* 138:2044–2049.

Krause, E., F. Pfeiffer, A. Scmid, and I. Schulz. 1996. Depletion of intracellular calcium stores activates a calcium conducting cation current in mouse pancreatic acinar cells. *J. Biol. Chem*. 271:32523–32528.

Kuno, M., J. Goronzy, C.M. Weyand, and P. Gardner. 1986. Single-channel and whole-cell recordings of mitogen-regulated inward currents in human cloned helper T lymphocytes. *Nature*. 323:269–273.

Lewis, R.S., and M.D. Cahalan. 1995. Potassium and calcium channels in lymphocytes. *Annu. Rev. Immunol.* 13:623–653.

Lewis, R.S., and M.D. Cahalan. 1989. Mitogen-induced oscillations of cytosolic $Ca^{2+}$ and transmembrane $Ca^{2+}$ current in human leukemic T cells. *Cell Reg.* 1:99–112.

Lichtenfels, R., W.E. Biddison, H. Schulz, A.B. Vogt, and R. Martin. 1994. CARE-LASS (calcein-release-assay), an improved fluorescence-based test system to measure cytotoxic T lymphocyte activity. *J. Immunol. Methods.* 172:227–239.

Luckhoff, A., and D.E. Clapham. 1994. Calcium channels activated by depletion of internal stores in A431 cells. *Biophys. J.* 67:177–182.

Negulescu, P.A., T.A. Krasieva, A. Khan, H.H. Kerschbaum, and M.D. Cahalan. 1996. Polarity of T cell shape, motility and sensitivity to antigen. *Immunity*. 4:421–430.

Ni, H.-T., M.J. Deeths, W. Li, D.L. Mueller, and M.F. Mescher. 1999. Signaling pathways activated by leukocyte function-associated Ag-1-dependent costimulation. *J. Immunol.* 162:5183–5189.

Parekh, A.B., and R. Penner. 1995. Depletion-activated calcium current is inhibited by protein kinase in RBL-2H3 cells. *Proc. Natl. Acad. Sci. USA*. 92: 7907–7911.

Parekh, A.B., and R. Penner. 1997. Store depletion and calcium influx. *Physiol. Rev*. 77:901–930.

Partiseti, M., F. Le Deist, C. Hivroz, A. Fischer, H. Korn, and D. Choquet. 1994. A calcium current activated by store depletion in human lymphocytes is absent in a primary immunodeficiency. *J. Biol. Chem*. 269:32327–32335.

Poenie, M., R.Y. Tsien, and A.-M. Schmitt-Verhulst. 1987. Sequential activation and lethal hit measured by $[Ca^{2+}]i$ in individual cytolytic T cells and targets. *EMBO (Eur. Mol. Biol. Organ.) J.* 6:2223–2232.

Premack, B.A., T.V. McDonald, and P. Gardner. 1994. Activation of calcium current in Jurkat T cells following the depletion of intracellular calcium stores by microsomal calcium-ATPase inhibitors. *J. Immunol.* 152:5226–5240.

Putney, J.W., Jr. 1990. Capacitative calcium entry revisited. *Cell Calcium*. 11: 611–624.

Sjaastad, M.D., R.S. Lewis, and W.J. Nelson. 1996. Mechanisms of integrin-mediated calcium signaling in MDCK cells: regulation of adhesion by IP3- and store-independent mechanisms. *Mol. Biol. Cell.* 7:1025–1041.

Steffenson, I.L., O.J. Mesna, E. Andruchow, E. Namork, K. Hylland, and R.A. Anderson. 1994. Cytotoxicity and accumulation of Hg, Ag, Cd, Cu, Pb, and Zn in human peripheral T and B lymphocytes and monocytes in vitro. *Gen. Pharmacol.* 25:1621–1633.

Takayama, H., G. Trenn, and M.V. Sitkovsky. 1987. A novel cytotoxic T lymphocyte activation assay: optimized conditions for antigen receptor triggered granule enzyme secretion. *J. Immunol. Methods.* 104:183–190.

Vaca, L., and D.L. Kunze. 1993. Depletion and refilling of intracellular $Ca^{2+}$ stores induce oscillations of $Ca^{2+}$ current. *Am. J. Physiol.* 264:H1319–H1322.

Wacholtz, M., E. Cragoe, and P. Lipsky. 1992. A $Na^{+}$-dependent $Ca^{2+}$ exchanger generates the sustained increase in intracellular $Ca^{2+}$ required for T cell activation. *J. Immunol.* 149:1912–1920.

Warnat, J., S. Phillip, S. Zimmer, V. Flockerzi, and A. Cavalie. 1999. Phenotype of a recombinant store-operated channel: highly selective permeation of calcium. *J. Physiol.* 518:631–638.

Weiss, A., and D.R. Littman. 1994. Signal transduction by lymphocyte antigen receptors. *Immunity*. 76:263–274.

Weismann, M., A.H. Guse, L. Sorokin, B. Broker, M. Friesr, R. Hallmann, and G.W. Mayr. 1997. Integrin-mediated intracellular calcium signaling in Jurkat T lymphocytes. *J. Immunol.* 158:1618–1627.

Yao, Y., and R. Tsien. 1997. Calcium current activated by depletion of calcium stores in *Xenopus* oocytes. *J. Gen. Physiol.* 109:703–715.

Zweifach, A., and R.S. Lewis. 1993. Mitogen-regulated $Ca^{2+}$ current of T lymphocytes is activated by depletion of intracellular $Ca^{2+}$ stores. *Proc. Natl. Acad. Sci. USA*. 90:6295–6299.

Zweifach, A., and R.S. Lewis. 1995. Slow calcium-dependent inactivation of depletion-activated calcium current ($I_{CRAC}$). Store-dependent and -independent mechanisms. *J. Biol. Chem*. 270:14445–14451.